

1-1-2015

## All-fiber mode-group-selective photonic lantern using graded-index multimode fibers

Bin Huang  
*University of Central Florida*

Nicolas K. Fontaine

Roland Ryf

Binbin Guan

Sergio G. Leon-Saval

*See next page for additional authors*

Find similar works at: <https://stars.library.ucf.edu/facultybib2010>

University of Central Florida Libraries <http://library.ucf.edu>

This Article is brought to you for free and open access by the Faculty Bibliography at STARS. It has been accepted for inclusion in Faculty Bibliography 2010s by an authorized administrator of STARS. For more information, please contact [STARS@ucf.edu](mailto:STARS@ucf.edu).

---

### Recommended Citation

Huang, Bin; Fontaine, Nicolas K.; Ryf, Roland; Guan, Binbin; Leon-Saval, Sergio G.; Shubochkin, R.; Shun, Y.; Lingle, R. Jr.; and Li, Guifang, "All-fiber mode-group-selective photonic lantern using graded-index multimode fibers" (2015). *Faculty Bibliography 2010s*. 6581.  
<https://stars.library.ucf.edu/facultybib2010/6581>

---

**Authors**

Bin Huang, Nicolas K. Fontaine, Roland Ryf, Binbin Guan, Sergio G. Leon-Saval, R. Shubochkin, Y. Shun, R. Lingle Jr., and Guifang Li

# All-fiber mode-group-selective photonic lantern using graded-index multimode fibers

Bin Huang,<sup>1,2</sup> Nicolas K. Fontaine,<sup>1,\*</sup> Roland Ryf,<sup>1</sup> Binbin Guan,<sup>1</sup> Sergio G. Leon-Saval,<sup>3</sup>  
R. Shubochkin,<sup>4</sup> Y. Sun,<sup>4</sup> R. Lingle Jr.,<sup>4</sup> and Guifang Li<sup>2</sup>

<sup>1</sup>Bell Laboratories/Alcatel-Lucent, 791 Holmdel Rd., Holmdel, NJ 07733, USA

<sup>2</sup>CREOL, The College of Optics and Photonics, University of Central Florida, Orlando, Florida 32816, USA

<sup>3</sup>Institute of Photonics and Optical Science (IPOS), School of Physics, The University of Sydney, Australia

<sup>4</sup>OFS, 2000 Northeast Expressway, Norcross, GA 30071, USA

\*nicolas.fontaine@alcatel-lucent.com

**Abstract:** We demonstrate the first all-fiber mode-group-selective photonic lantern using multimode graded-index fibers. Mode selectivity for mode groups  $LP_{01}$ ,  $LP_{11}$  and  $LP_{21} + LP_{02}$  is 20-dB, 10-dB and 7-dB respectively. The insertion loss when butt coupled to multimode graded-index fiber is below 0.6-dB. The use of the multimode graded-index fibers in the taper can significantly reduce the adiabaticity requirement.

©2015 Optical Society of America

OCIS codes: (060.2340) Fiber optics components, (060.2330) Fiber optics communications.

---

## References and links

1. R.-J. Essiambre, G. Kramer, P. J. Winzer, G. J. Foschini, and B. Goebel, "Capacity limits of optical fiber networks," *J. Lightwave Technol.* **28**(4), 662–701 (2010).
2. D. J. Richardson, J. M. Fini, and L. E. Nelson, "Space division multiplexing in optical fibers," *Nat. Photonics* **7**(5), 354–362 (2013).
3. R. Ryf, S. Randel, A. H. Gnauck, C. A. Bolle, A. Sierra, S. Mumtaz, M. Esmaelpour, E. C. Burrows, R.-J. Essiambre, P. J. Winzer, D. W. Peckham, A. McCurdy, and R. Lingle, "Mode-division multiplexing over 96 km of few-mode fiber using coherent  $6 \times 6$  MIMO processing," *J. Lightwave Technol.* **30**(4), 521–531 (2012).
4. N. Bai, E. Ip, Y.-K. Huang, E. Mateo, F. Yaman, M.-J. Li, S. Bickham, S. Ten, J. Liñares, C. Montero, V. Moreno, X. Prieto, V. Tse, K. Man Chung, A. P. T. Lau, H.-Y. Tam, C. Lu, Y. Luo, G.-D. Peng, G. Li, and T. Wang, "Mode-division multiplexed transmission with inline few-mode fiber amplifier," *Opt. Express* **20**(3), 2668–2680 (2012).
5. R. Ryf, R. Essiambre, A. Gnauck, S. Randel, M. A. Mestre, C. Schmidt, P. Winzer, R. Delbue, P. Pupalakis, A. Sureka, T. Hayashi, T. Taru, and T. Sasaki, "Space-division multiplexed transmission over 4200 km 3-core microstructured fiber," in *Optical Fiber Communication Conference*, OSA Technical Digest (Optical Society of America, 2012), paper PDP5C.2.
6. B. Zhu, T. F. Taunay, M. Fishteyn, X. Liu, S. Chandrasekhar, M. F. Yan, J. M. Fini, E. M. Monberg, and F. V. Dimarcello, "112-Tb/s space-division multiplexed DWDM transmission with 14-b/s/Hz aggregate spectral efficiency over a 76.8-km seven-core fiber," *Opt. Express* **19**(17), 16665–16671 (2011).
7. J. Sakaguchi, Y. Awaji, N. Wada, A. Kanno, T. Kawanishi, T. Hayashi, T. Taru, T. Kobayashi, and M. Watanabe, "109-Tb/s (7x97x172-Gb/s) SDM/WDM/PDM QPSK transmission through 16.8-km homogeneous multicore fiber," in *Optical Fiber Communication Conference/National Fiber Optic Engineers Conference 2011*, OSA Technical Digest (CD) (Optical Society of America, 2011), paper PDPB6.
8. N. K. Fontaine, R. Ryf, J. Bland-Hawthorn, and S. G. Leon-Saval, "Geometric requirements for photonic lanterns in space division multiplexing," *Opt. Express* **20**(24), 27123–27132 (2012).
9. B. Huang, C. Xia, G. Matz, N. Bai, and G. Li, "Structured directional coupler pair for multiplexing of degenerate modes," in *Optical Fiber Communication Conference/National Fiber Optic Engineers Conference 2013*, OSA Technical Digest (online) (Optical Society of America, 2013), paper JW2A.25.
10. N. Riesen and J. D. Love, "Weakly-guiding mode-selective fiber couplers," *Quantum Electronics, IEEE Journal of* **48**(7), 941–945 (2012).
11. N. Riesen, J. D. Love, and J. W. Arkwright, "Few-core spatial-mode multiplexers/demultiplexers based on evanescent coupling," *Photonics Technology Letters, IEEE* **25**(14), 1324–1327 (2013).
12. R. Ryf, N. K. Fontaine, M. Montoliu, S. Randel, B. Ercan, H. Chen, S. Chandrasekhar, A. Gnauck, S. G. Leon-Saval, J. Bland-Hawthorn, J. R. Salazar Gil, Y. Sun, and R. Lingle, "Photonic-lantern-based mode multiplexers for few-mode-fiber transmission," in *Optical Fiber Communication Conference*, OSA Technical Digest (online) (Optical Society of America, 2014), paper W4J.2.

13. S. G. Leon-Saval, N. K. Fontaine, J. R. Salazar-Gil, B. Ercan, R. Ryf, and J. Bland-Hawthorn, "Mode-selective photonic lanterns for space-division multiplexing," *Opt. Express* **22**(1), 1036–1044 (2014).
14. N. K. Fontaine, S. G. Leon-Saval, R. Ryf, J. R. Salazar Gil, B. Ercan, and J. Bland-Hawthorn, "Mode selective dissimilar fiber photonic-lantern spatial multiplexers for few-mode fiber," in *Proceedings of European Conference on Optical Communication (2013)*, paper PD1.C.3.
15. S. Yerolatsitis, I. Gris-Sánchez, and T. A. Birks, "Adiabatically-tapered fiber mode multiplexers," *Opt. Express* **22**(1), 608–617 (2014).
16. C. Xia, A. M. Velazquez-Benitez, X. Liu, J. E. Antonio-Lopez, H. Wen, B. Zhu, R. Amezcua-Correa, and G. Li, "Demonstration of world's first few-mode GPON" in *Proceedings of European Conference on Optical Communication (2014)*, paper PD.1.5.
17. R. Ryf, N. K. Fontaine, B. Guan, B. Huang, M. Esmacelpour, S. Randel, A. H. Gnauck, S. Chandrasekhar, A. Adamecki, G. Raybon, R. W. Tkach, R. Shubochkin, Y. Sun, and R. Lingle, Jr., "305-km combined wavelength and mode-multiplexed transmission over conventional graded-index multimode fibre." in *Proceedings of European Conference on Optical Communication (2014)*, paper PD.3.5.
18. A. W. Snyder and J. D. Love, *Optical Waveguide Theory* (Chapman & Hall, 1983), pp.407–413.
19. N. K. Fontaine, "Characterization of multi-mode fibers and devices for MIMO communications". Proc. SPIE 9009, *Next-Generation Optical Communication: Components, Sub-Systems, and Systems III*, 90090A.
20. N. Fontaine, R. Ryf, M. Mestre, B. Guan, X. Palou, S. Randel, Y. Sun, L. Gruner-Nielsen, R. Jensen, and R. Lingle, "Characterization of space-division multiplexing systems using a swept-wavelength interferometer," in *Optical Fiber Communication Conference/National Fiber Optic Engineers Conference 2013*, OSA Technical Digest (online) (Optical Society of America, 2013), paper OW1K.2.

## 1. Introduction

In recent years, the transmission capacity of a single mode fiber has been rapidly approaching its theoretical limits [1]. For further capacity growth, space-division multiplexing (SDM) which utilizes multiple spatial modes can address this capacity crunch [2]. Transmission in few mode fibers (FMFs), multi-mode fibers (MMF), and multicore fibers (MCFs) have been demonstrated experimentally [3–7]. A SDM transmission system consists of an array of transmitters, a spatial multiplexer (SMUX) to launch onto the SDM fiber's modes or cores, a SDM fiber, a spatial demultiplexer (SDeMUX), an array of coherent receivers, and multiple-input multiple-output (MIMO) processing to undo mode mixing. SMUXes and SDeMUXes are a key components for SDM.

Fiber-based photonic lanterns (PLs), in which multiple optical fibers are adiabatically transformed into a single MMF, are a promising candidate for S(De)MUXes as they provide low insertion loss and low mode dependent loss if the PL is adiabatically tapered and packed optimally. Optimal packing structures for photonic lanterns have been discussed in detail in [8]. Also, the bandwidth of the PLs are broad and can easily cover the entire C-band and L-band. Unlike directional couplers [9–11] whose bandwidth is limited by the phase-matching condition, the PL has weak wavelength dependence as adiabaticity is only weakly dependent on wavelength. PLs can also be scaled to a large number of modes.

Most photonic-lantern-based S(De)MUXes use single-mode input (output) fibers. Symmetric PLs, in which all input/output single-mode fibers are identical, are non-mode-selective as there is no one-to-one correspondence between an input/output fiber and a specific mode of the input/output MMF. WDM transmission using non-mode-selective PLs over 900 km has also been demonstrated [12]. PLs can have mode-selectivity if the multiple input/output fibers are different. Mode-selective photonic lanterns supporting three modes have already been demonstrated [13–15]. Mode-selective PLs can find applications for SDM transmission in FMFs with low mode crosstalk such as time-division multiplexed (TDM) passive optical networks (PON) [16]. For long-distance transmission in low-crosstalk FMFs, mode-selective PLs can be used to compensate differential modal group delay (DMGD) [14,17]. Because degenerate modes in MMFs and FMFs strongly couple with each other, it is not necessary to make the photonic lantern selective between degenerate modes in the same group. In other words, mode-group-selective (MGS)-PLs are adequate for the above-mentioned applications. For example, Fig. 1 shows a DMGD compensator. The DMGD compensator demultiplexes a mode-division multiplexed signal using a MGS-PL, equalizes the delay between mode groups using fiber delays, and remultiplexes using another MGS-PL.

The graded index (GI)-MMF in Fig. 1 can support 6 spatial modes (12 if polarization is considered) and the 6 spatial modes can be divided into 3 mode groups, group 1 ( $LP_{01}$ ), group 2 ( $2 \times LP_{11}$ ) and group 3 ( $2 \times LP_{21} + LP_{02}$ ). The spatial modes within each group are nearly degenerate with approximately equal group velocity. In [17], DMGD compensation using two MGS-PLs was demonstrated experimentally to reduce MIMO complexity in 305-km transmission over a GI-MMF with a spectral-efficiency-distance product of 2745 bit/s/Hz km. In depth analysis of these MGS-PLs are shown in this paper.

Here, we report a new method to fabricate MGS-PLs. The key innovation is the use of multi-mode instead of single-mode fibers for the taper, in particular graded-index multimode fibers (GI-MMFs). As will be explained in Section 2, the introduction of MMF cannot only achieve high mode selectivity but also relax the requirement for adiabaticity. Section 3 and 4 present simulation and experimental results of the GI-MMF-based MGS-PL.

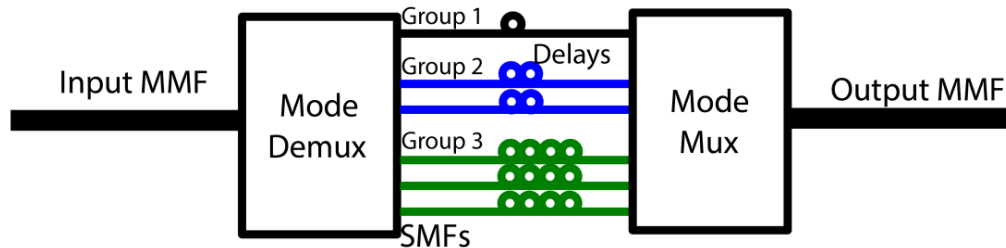


Fig. 1. Differential group delay compensator for the first three mode-groups of a GI-MMF.

## 2. Rationale for employing graded-index MMF

The structure of a photonic lantern is shown in Fig. 2. A PL-based multiplexer consists of  $M$  individual fibers with a core of index  $n_{2,m}$  and core diameter  $r_m$  surrounded by a cladding with refractive index  $n_{1,m}$  that are packed into a capillary made of fluorine-doped silica with a refractive index  $n_0$  that is lower than the fiber cladding. The entire structure is then adiabatically tapered. During the taper, light that is initially confined in the individual cores escape as the cores shrink. The escaped light is captured and guided by the cladding and low-index capillary. At the end of the taper, each core is so small that they have little effect on the output modes of the PL, and the light is now guided by the core made of the fiber cladding material with the low-index capillary as the new cladding.

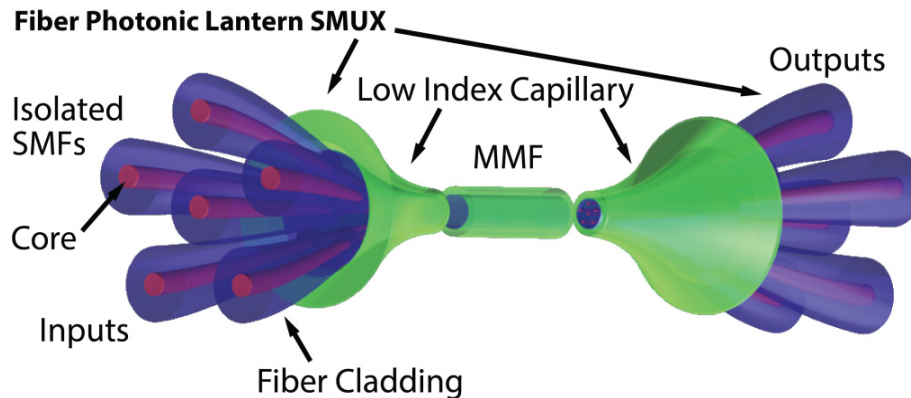


Fig. 2. Fiber photonic lantern based SMUX.

When the individual fibers are identical,  $n_{2,i} = n_{2,j}$  and  $r_i = r_j$ , the PLs are non-mode selective. Launching light into any individual fiber core will excite a combination of modes at the lantern output. This is because all the modes couple strongly at the beginning of the taper since they have the same propagation constant. Mode-selective lanterns can be made if  $n_{2,i} \neq n_{2,j}$  and/or  $r_i \neq r_j$ . Dissimilar fibers break the degeneracy of the local modes of the lantern throughout the entire taper and force each input core to map to each mode of the output MMF. Symmetry can be selectively preserved for degenerate modes in the same mode group of the output fiber of the PL. In this case, the PL is mode-group selective. Demonstrations of a MGS-PL for the  $LP_{01}$  mode and the  $LP_{11}$  mode group have verified this concept [14, 16]. In [14], a SMF with a higher effective index was mapped onto the  $LP_{01}$  output mode and two SMFs with a lower effective index were mapped onto the  $LP_{11}$  output mode group.

The ability for the PL to scale to more mode groups is very desirable for high-capacity SDM transmission systems. Theoretically for MGS-PLs, there is no restriction in terms of scalability, provided that the adiabaticity criterion is satisfied in the taper transition, given by [15, 18]:

$$\left| \frac{2\pi}{\beta_1 - \beta_2} \frac{d\rho}{dz} \int \psi_1 \frac{\partial \psi_2}{\partial \rho} dA \right| \ll 1 \quad (1)$$

where  $\Psi_1$  and  $\Psi_2$  are the normalized field distribution of the local modes that are likely to couple to each other,  $\beta_1$  and  $\beta_2$  are their respective propagation constants,  $\rho$  is the local core radius,  $z$  is the longitudinal distance along the PL,  $A$  is the cross-sectional area of the PL. The first term of Eq. (1) dictates that the tapering rate  $\frac{d\rho}{dz}$  is inversely proportional to the differences in the propagation constants of the two modes (i.e., propagation constant criterion). The second terms of Eq. (1) suggests that mode profiles that change slowly as the fiber is tapered will lead to low crosstalk (i.e., mode profile criterion). It was argued in [15] that each of these two effects requires tapering length to increase linearly with  $N$  and therefore the combined effect requires the tapering length to increase approximately as  $N^2$ . In [15], reduced-cladding SMFs, which has much slower change of the mode field diameter as it is tapered, was used to satisfy the adiabaticity requirement via the mode profile criterion.

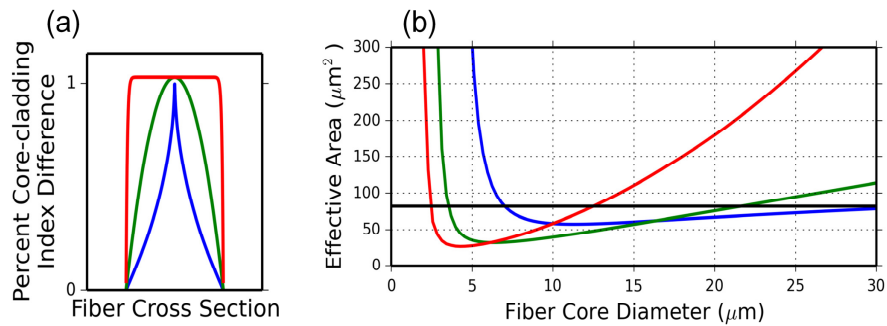


Fig. 3. (a) Refractive index profile of MMFs. Step index MMF (red),  $\alpha = 2$  graded index MMF (green),  $\alpha = 0.5$  graded index MMF (blue). (b) Effective area of the fundamental mode of different fibers in the taper. Step index MMF (red),  $\alpha = 2$  graded index MMF (green),  $\alpha = 0.5$  graded index MMF (blue). The black line represents the effective area of SSMF ( $80 \mu\text{m}^2$ ).

In this paper, we propose to use GI-MMFs to satisfy the adiabatic requirement via both the propagation constant criterion and the mode profile criterion. In addition, we use GI-MMF to improve splice loss between the input SMFs and the lantern. To improve the propagation constant criterion, large difference of  $(\beta_1 - \beta_2)$  will greatly reduce the adiabaticity requirement. Dissimilar MMFs as input fibers offer a much larger range of propagation constant differences between their fundamental modes than what dissimilar SMFs allow. Propagation constant differences between dissimilar SMFs are constrained by the available core diameter and refractive index to maintain single-mode operation. To improve the mode-profile criterion, we use GI-MMFs because the mode changes slower than that of the step-index MMF, which will be discussed in the following paragraph.

The use of multimode fiber for the input/output PL S(De)MUX is practical for two reasons. First, when the length of the MMF is short, mode coupling to higher-order modes of the MMF is negligible. Second, standard SMFs (SSMFs) can be coupled to the fundamental mode of GI-MMFs with low splice-loss even if the diameter of the dissimilar GI-MMFs varies. The effective area of the fundamental mode of the GI-MMF can be designed to be approximately equal to SSMF for a wide range of core diameters. Figure 3(a) shows the refractive index profile of three types of MMFs [step-index MMF (red), GI-MMF with  $\alpha = 2$  (green) and  $\alpha = 0.5$  (blue)]. Figure 3(b) displays the effective areas of the fundamental mode of these fibers as a function of core diameter. The core-cladding index contrast is set to 1%. From Fig. 3(b), two advantages of GI-MMF compared to step-index MMFs are apparent: 1) the effective area of the GI-MMFs changes much slower than step-index MMFs as the core diameter varies which better satisfies the mode-profile criterion, and 2) the effective area of GI-MMF with  $\alpha = 2$ , almost matches the SSMF ( $80\mu\text{m}^2$ ) over a wide range of core diameters between  $15\mu\text{m}$  and  $25\mu\text{m}$ , which results in low splice loss. Changing  $\alpha$  and the core-cladding index contrast can further optimize the splice loss between GI-MMFs and the external SSMF. Finally, GI-MMFs with  $125\mu\text{m}$  claddings are easier to handle than reduced cladding fibers.

### 3. Simulation results

From discussions above, selection of dissimilar GI-MMFs is critical to building a MGS-PL. The selection rules are two-fold. First, the difference of propagation constants between fundamental modes corresponding to the output mode groups should be as large as possible to make adiabatic tapering robust. For MGS PLs using GI-MMFs, the fundamental mode launched into an individual core maps to the corresponding lantern mode, while higher order modes in an individual core couple to the cladding modes (guided by the capillary) that eventually becomes radiative. Another constraint is that the effective index of the modes should not cross or interact with each other during the taper. To be more specific, the effective index of the fundamental mode of each GI-MMF must be larger than that of any higher order mode in any of the input fibers.

Figure 4 shows a simulation using input fibers that meet those selection rules for a three mode group MGS-PL. Figure 4(a) shows the fiber cross section. The input fiber at the center is a  $22\mu\text{m}$ -core-diameter GI-MMF for exciting the  $LP_{01}$  output mode (group 1), the two  $20\mu\text{m}$ -core-diameter GI-MMFs excite the two  $LP_{11}$  modes (group 2) and the three  $15\mu\text{m}$ -core-diameter GI-MMFs excite the three nearly-degenerate  $LP_{21} + LP_{02}$  modes (group 3). The index contrast of the GI-MMF in the simulation is 1%. The claddings have diameters of  $125\mu\text{m}$ . In Fig. 4(b), the effective indexes of the 3 mode groups of interest (1-black, 2-blue, 3-green) and other higher order mode groups (red) of the individual fibers that become cladding modes are plotted as functions of the taper ratio. It is noted that the effective index of the higher-order modes are smaller than that of any of the fundamental modes of the 6

dissimilar fibers, ensuring no resonant coupling occurs between a high-order mode from one input fiber to a fundamental mode of another fiber.

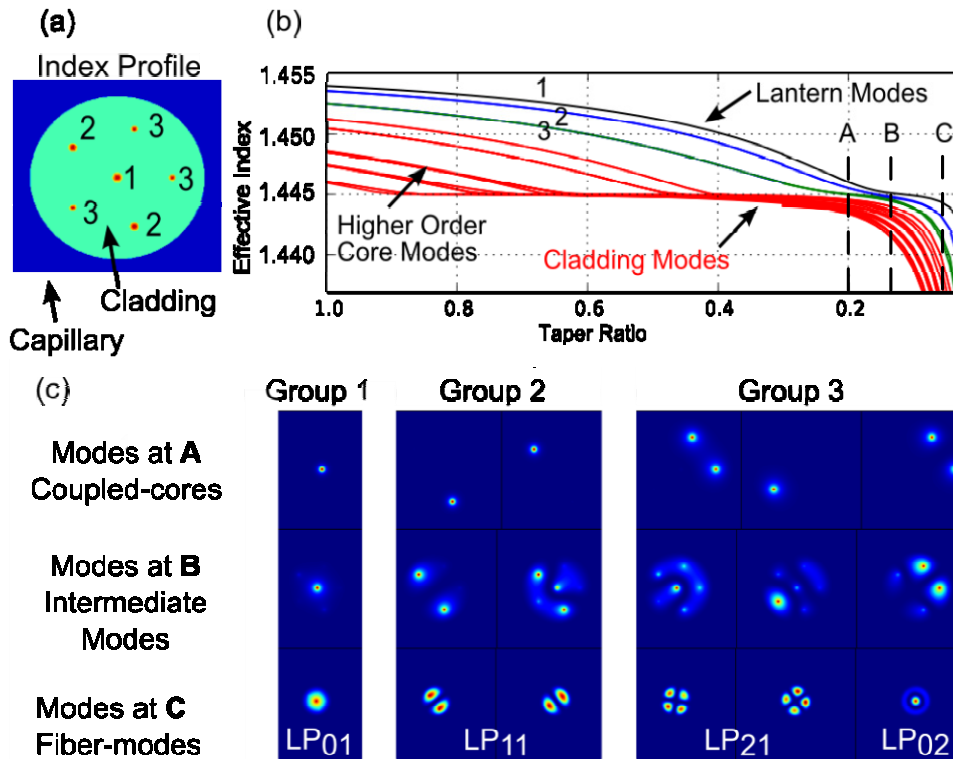


Fig. 4. (a) Six-fiber lantern index profile with 3 types of dissimilar cores (1, 2 and 3). (b) Propagation constants and (c) intensity of the modes at different stages of the taper.

At a taper ratio around 0.9, the highest-order modes of each fiber begin to couple to the cladding modes (guided by capillary). At a taper ratio around 0.4, all the higher order modes are coupled to the cladding modes of the PL, while the fundamental modes are still guided by individual cores. If the effective index of any higher-order mode were larger than that of one of the fundamental modes, the effective indexes of these two modes will cross each other in the taper region before the higher order mode finally couples to the cladding mode. Near the cross point, the effective indexes of these two modes are almost the same and mode coupling will occur. As a result, the signal in that fundamental mode would couple to the higher order modes and finally be lost to the cladding mode, leading to mode dependent loss of the mode selective lantern.

Figure 4(c) depicts the intensity patterns of the PL modes at different points in the taper region. For taper ratios from 1 to 0.2 (region before A), the cores are brought closer together but the lantern modes are still well confined within the GI-MMF cores. At B (taper ratio = 0.15), the cores begin to couple strongly to each other. At C (taper ratio around 0.11), the cores become small enough that the PL modes appear in the MMF composed of the fused-cladding core and capillary cladding. After C, the cores become so small that they have negligible effect on the PL modes and the structure can be tapered to desired dimensions. The transition between A and C (especially around B) is the most sensitive because the mode profiles change significantly as the photonic-lantern modes transition from core-guiding and



cladding-guiding. As a result, the taper speed in fabrication could be fast for taper ratios from 1.0 to A and should be slow between points A and C.

#### 4. Experimental results

**Table 1. Parameters of mode group selective lanterns.**

	2-mode group selective lantern	3-mode group selective lantern
Fiber for $LP_{01}$ mode (mode group 1)	20 $\mu\text{m}$ GI-MMF	22 $\mu\text{m}$ GI-MMF
Fiber for $LP_{11}$ modes (mode group 2)	15 $\mu\text{m}$ GI-MMF	20 $\mu\text{m}$ GI-MMF
Fiber for $LP_{21} + LP_{02}$ modes (mode group 3)		15 $\mu\text{m}$ GI-MMF
Taper Ratio	8.5	11.2
Final Diameter	27 $\mu\text{m}$	29 $\mu\text{m}$

Table 1 shows detailed construction of GI-MMF-based MGS-PL supporting 2 and 3 mode groups. The GI-MMFs are selected such that the effective indices between the fundamental mode and the higher order modes do not cross. Figure 5(a) and Fig. 5(b) shows the end facet and the near-field output mode profiles of the fabricated two mode group MGS-PL. High selectivity is observed between these two mode groups. As expected, for the degenerate  $LP_{11}$  mode groups, a ring-like intensity profile representing linear combination of the two  $LP_{11}$  modes exhibits high selectivity to  $LP_{01}$  mode. Figure 6(a) and Fig. 6(b) show the end facet and near-field output intensity profiles of a three mode group MGS-PL. Three mode groups can be clearly observed. The tapered end of the PL is butt coupled to a 50- $\mu\text{m}$  core diameter GI-MMF. Figure 5(c) and Fig. 6(c) show the output field at the end of a 50-m GI-MMF which indicates qualitatively that the desired mode groups have been excited using the MGS-PLs.

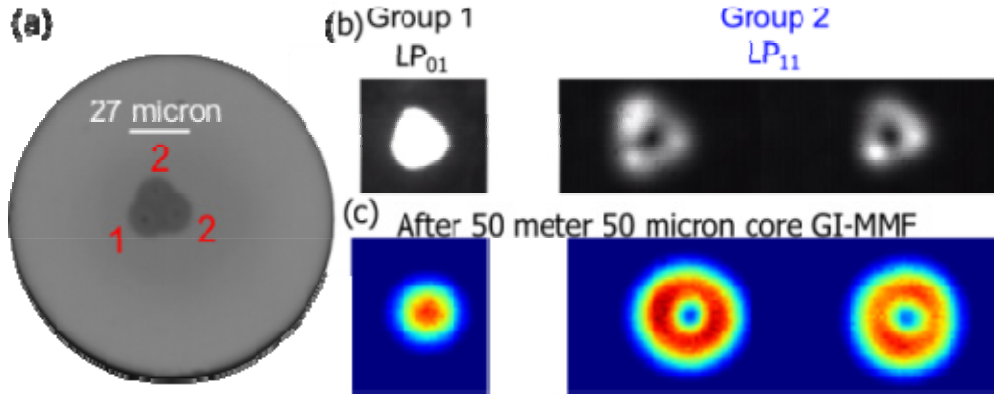


Fig. 5. (a) End facet of the mode group selective lantern supporting two mode groups. (b) Near field intensity profile. (c) Intensity profiles after 50-m of GI-MMF when illuminated with a C-band broadband source.

Next, we measured the insertion loss and quantitatively characterized the mode selectivity. Insertion loss (including splicing and butt coupling to the GI-MMF transmission fiber) is measured to be less than 0.6 dB for both MGS-PLs. To characterize mode selectivity we use a swept-wavelength interferometer (SWI) with spatial-diversity operating in reflection mode to measure the transfer matrix across the entire C-band [19,20]. The system measurement is from the SMF inputs fusion spliced to the input GI-MMFs, through the PL, 50-meter output GI-MMF, cleaved facet of the output GI-MMF, then back through 50-meter

GI-MMF, PL and to the SMF. The 50-m GI-MMF introduces modal group delays by which the mode groups can be separated. The MGS-PL acts both as a multiplexer and a demultiplexer in these measurements. Thus, the mode selectivity is characterized for the system that comprises a multiplexer, GI-MMF and a demultiplexer.

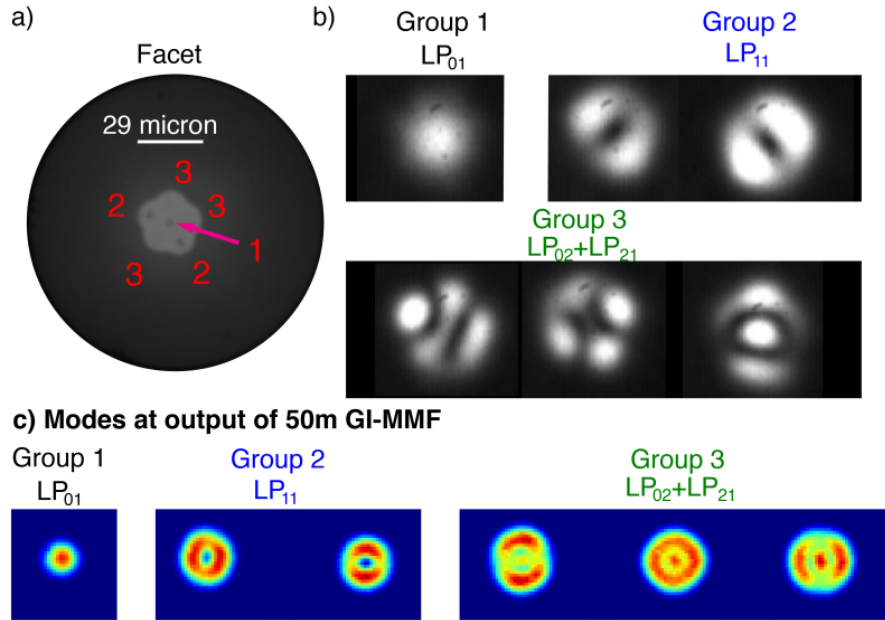


Fig. 6. (a) End facet of the mode group selective lantern supporting three mode groups. (b) Near field mode profile. (c) Mode profiles after 50-m of GI-MMF when illuminated with a C-band broadband source.

The time-domain transfer matrix for the three mode group MGS-PL is shown in Fig. 7 and contains 36 cells. The transfer matrix for a two mode group MGS-PL would contain only 9 cells and is shown as a subset of the three mode group MGS-PL transfer matrix. The columns correspond to the received ports, and the rows to the launched ports. The 50-m GI-MMF contains 8 degenerate mode groups and each group has a unique group delay. Therefore, the time-domain impulse responses can have 8 mode-peaks. The first 3 peaks correspond to group 1, group 2, and group 3 and the last 5 peaks correspond to higher-order-mode (HOM) groups. For a MGS-PL with high mode selectivity, light launched into the fibers in mode group I ( $I = 1, 2, 3$ ) should be received on the fibers for mode group I. In addition, the majority of the power should be contained in the mode-peak mode groups DGD. These 'signal' cells are on the diagonal and form a  $1 \times 1$  block for the first group (gray cell), a  $2 \times 2$  block for the second group (blue cells), and a  $3 \times 3$  block for the third group (green cells). The energy that does not couple into these cells are crosstalk (red cells). Additionally, the mode peaks indicate which modes are causing crosstalk.

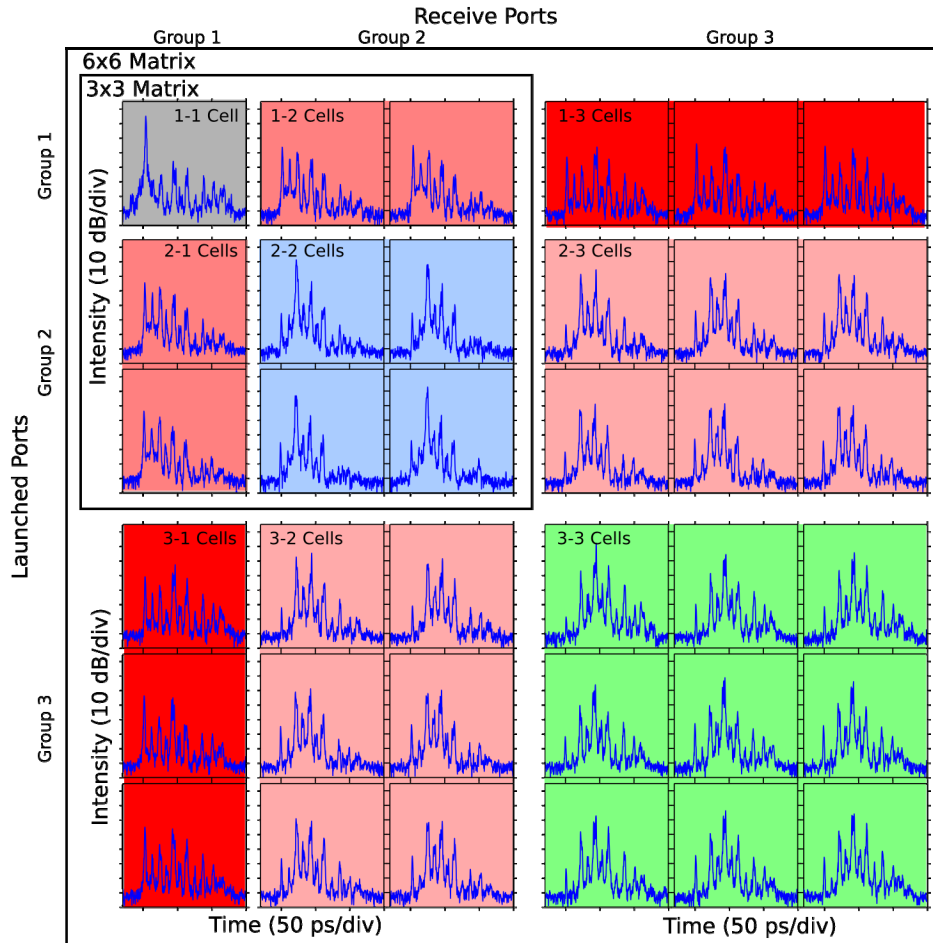


Fig. 7. Full transfer matrix for the three mode-group MGS-PL (6 spatial modes). Crosstalk between groups are indicated by red cells. Cell blocks on the diagonal are the signal cells. The two mode group MGS-PL matrix is a subset of the  $6 \times 6$  matrix.

The MGS-PL supporting two mode groups has a transfer matrix that contains 9 elements. The full transfer matrix is not shown, but it would be similar to the 3x3 matrix in Fig. 7. To quantify mode selectivity we can find the total signal power received in mode group I by summing the ‘signal’ cells together. The total crosstalk on group I is the summation of the crosstalk cells in the columns corresponding to mode group I. The mode-selectivity for mode group I is defined as the ratio of the crosstalk on group I to the signal power received in mode group I. Figure 8 shows these summations. The 1-1 cell shows the clean excitation of the  $LP_{01}$  mode with suppression of the HOMs (e.g., the additional mode peaks). The 2-2 summation (e.g., blue cells in Fig. 7) shows excitation of the  $LP_{11}$  modes with 40-dB rejection of the  $LP_{01}$  mode, and about 18-dB rejection of the  $LP_{21} + LP_{02}$  modes. The 1-2 summation (1-2 cells in Fig. 8) shows the total crosstalk between groups, and is roughly 18-dB smaller than the signals. These measurements show that MGS-PL supporting two mode groups has 20-dB mode selectivity for mode group 1 and 2 into the GI-MMF.

## System crosstalk matrix elements

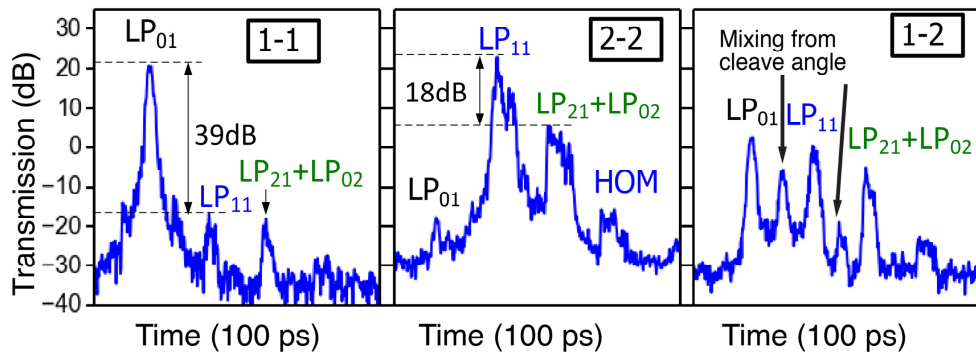


Fig. 8. Summation of signal and crosstalk cells from the reflection transfer matrix for mode group selective lantern supporting two mode groups.

Next, we analyze the MGS-PL supporting three groups. Figure 9 shows the signal cells and the crosstalk cells. The 1-1 cell shows excitation of only the  $LP_{01}$  with 31-dB suppression of the mode group  $LP_{21} + LP_{02}$  which has the largest crosstalk among all the undesired modes. The 2-2 cell shows excitation of the  $LP_{11}$  modes with 40-dB rejection of the  $LP_{01}$  mode and 16-dB rejection of the  $LP_{21} + LP_{02}$  modes. The 3-3 cell shows excitation of the  $LP_{21} + LP_{02}$  modes with 35-dB rejection of the  $LP_{01}$  mode, 13-dB rejection of the HOM (fourth peak), and 15-dB rejection of the  $LP_{11}$  modes. The mode selectivity is 20-dB, 10-dB and 7-dB for groups 1, 2 and 3, respectively.

## System crosstalk matrix elements

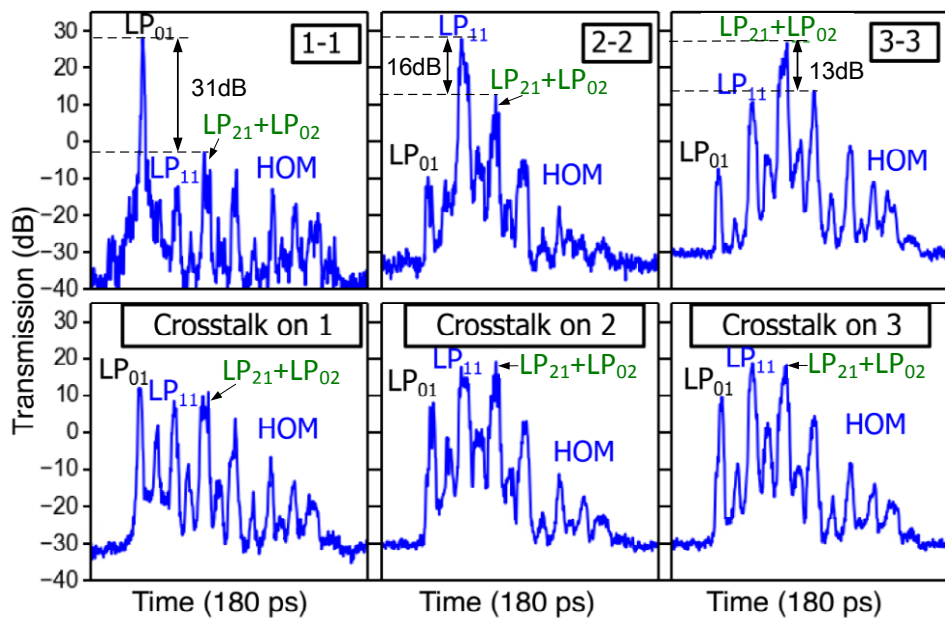


Fig. 9. Summation of signal and crosstalk cells from reflection transfer matrix for mode group selective lantern supporting three mode groups.

## 5. Conclusion

We have demonstrated all-fiber mode-group-selective PL with low insertion loss and high mode-group selectivity. The insertion loss (including splicing) of these PL is less than 0.6-dB. The mode selectivity for the mode-group-selective PL is 20-dB which is much better than the modal crosstalk in a typical 50-km fiber span (7-dB). Furthermore, we have demonstrated a mode-group-selective PLs with mode selectivity of 20-dB, 10-dB and 7-dB for mode groups  $LP_{01}$ ,  $LP_{11}$ , and  $LP_{21} + LP_{02}$ . The mode selectivity can be improved further by optimizing the mode field matching between the PL and the transmission MMF. The use of GI-MMFs was a key to reduce the device insertion loss and reduce the adiabaticity requirement.

## Acknowledgments

The authors thank the support by the IT R&D program of MKE/KEIT [10043383, Research of Mode-Division-Multiplexing Optical Transmission Technology over 10km Multi-Mode Fiber] and the National Basic Research Program of China (973) Project #2014CB340100 and NSFC Project (61307085).